applied sciences

MDPI

Article

The Sinkhole Phenomenon—Changes in Compartment Fire Characteristics Due to Incomplete Combustion before Flame Ejection

Hong-Seok Yun [1], Sun-Yeo Mun [2] and Cheol-Hong Hwang [1,*]

[1] Department of Fire and Disaster Prevention, Daejeon University, Daehak-ro 62, Daejeon 34520, Republic of Korea
[2] Department of Disaster Prevention, Graduate School, Daejeon University, Daehak-ro 62, Daejeon 34520, Republic of Korea
* Correspondence: chehwang@dju.ac.kr

Abstract: In this study, experiments and numeric studies were conducted to analyze the causes of abnormal behavior in temperature, heat flux, and combustion efficiency that occurred before a compartment fire was converted to the under-ventilated condition. The fire experiments were performed using a 1/4 reduced-scale ISO 9705 compartment and propane fuel. Considering that the occurrence and termination of abnormal behavior are related to ventilation conditions, vertical openings of various shapes designed to have the identical ventilation factor ($0.52A\sqrt{h}$) were used. As a result, an abnormal phenomenon was observed in which the measured heat release rate did not increase despite the increase in the fuel flow rate under the over-ventilation condition in all opening shapes. Due to this phenomenon, the combustion efficiency was reduced to 70% regardless of the opening shape. In order to understand these abnormal behaviors and to analyze the causes of their occurrence, the temperature and chemical species concentrations of the opening discharge flow were measured. The results indicated that the abnormal behavior of thermal physical quantities, HRR, and combustion efficiency occurred because fuel that was not burned inside the compartment did not reach the lower combustion limit even outside the compartment and was discharged.

Keywords: compartment fire; ventilation condition; combustion efficiency; global equivalence ratio; fire behavior

check for updates

Citation: Yun, H.-S.; Mun, S.-Y.; Hwang, C.-H. The Sinkhole Phenomenon—Changes in Compartment Fire Characteristics Due to Incomplete Combustion before Flame Ejection. *Appl. Sci.* **2022**, *12*, 12278. https://doi.org/10.3390/app122312278

Academic Editor: Francesca Scargiali

Received: 28 October 2022
Accepted: 28 November 2022
Published: 30 November 2022

1. Introduction

Thermal feedback from the heated wall and smoke layer in the compartment fire environment promotes thermal decomposition of combustibles. The increase in fuel supply causes incomplete combustion due to insufficient oxygen and an increase in the yield of toxic substances (e.g., soot and carbon monoxide) [1,2]. When the oxygen inside the compartment is continuously reduced, the fire transitions to the under-ventilated condition, and flames are ejected through openings. Flame ejection through openings can increase damage to life and property as the fire spreads to upper floors and adjacent spaces [3–5]. Therefore, the start time of an under-ventilated fire is regarded as important information for assessing the risk of compartment fires. Even under the same combustible conditions, the initiation time of an under-ventilated fire may vary depending on the air inflow rate of the opening. As such, changes in fire characteristics according to ventilation conditions are of major interest in fire engineering, and many studies on this are underway [6–11].

As part of the literature on fire characteristics, studies [12–14] were performed to evaluate the effects of fuel type and distribution and opening size on fire characteristics. In these studies, fire characteristics according to various variables were investigated. In addition, thermal physical quantities different from those commonly known were observed during this process. It is known that the gas temperature in the compartment under pre-flashover fire conditions is proportional to the HRR [15]. However, in these studies [12–14], the upper layer temperature (ULT) and incident heat flux were not proportional to HRR in the fire growth stage. Specifically, in studies by Lock et al. [12] and Hwang et al. [13] that used ISO 9705 [16], the ULT and incident heat flux on the floor temporarily decreased despite the increase in HRR due to the boiling of liquid fuel, and then increased afterwards. Similarly, in the study by Parkes [14], the ULT was constant at approximately 250 °C despite the increase in HRR from 450 kW to 650 kW. After the transient abnormal behavior, ULT increased rapidly, showing behavior proportional to HRR. The HRR measured in the section where this phenomenon was observed was considerably lower than the ideal HRR. Considering this, it can be inferred that incomplete combustion is the cause of the abnormal thermal physical quantities. Incomplete combustion in the fire growth stage can increase the fire risk by generating more toxic substances than expected. However, the causes and effects of this phenomenon, which appears very temporarily, have not been analyzed in detail. Therefore, it is necessary to better understand it by analyzing the fire behavior of compartment fires that grow in stages.

Staged fire growth can be implemented using the concept of global equivalence ratio (GER, ϕ_g). GER, a concept similar to the equivalence ratio of a premixed flame, can be used to quantify the ventilation condition of a compartment fire assuming the complete mixing of fuel/air in the compartment from a macroscopic perspective. Fuel is locally mixed and diffused with the air in an actual compartment, so GER calculated based on the assumption of complete mixing may differ from the actual value. Nevertheless, GER can be used to predict CO yield through the fuel-specific correlation that varies with the ULT [17,18]. Hwang et al. [19] examined chemical species concentrations and ULT in the range of ϕ_g = 0.5~3.0 under various ventilation conditions in ISO 9705 and confirmed that the chemical species concentration and ULT had a linear relationship with GER, and the predictability through correlation was suggested. In addition, Ko et al. [20] investigated local and global combustion efficiency according to GER to analyze fire phenomena. These studies demonstrate that the GER concept is effective for analyzing the phenomena of fires that grow in stages.

Yamada et al. [21] examined compartment fire phenomena by analyzing combustion efficiency according to GER and reported a decrease in combustion efficiency in the over-ventilated condition (ϕ_g < 1.0). The combustion efficiency continued to decrease from ϕ_g = 0.75 to the condition of ϕ_g = 1.27 where the flame was ejected. After flame ejection, the combustion efficiency increased with GER, showing a value close to 100%. Lee et al. [22] and Ukleja et al. [23] also observed this phenomenon; they reported that the CO yield rapidly increased in the section where the combustion efficiency decreased. Researchers have named this phenomenon "plateau" and "under-ventilated condition," but the causes of this abnormal behavior have not been analyzed. In Parkes's study [14] mentioned above, the abnormal behavior of ULT occurred in the range of ϕ_g = 0.6~1.2, similar to the findings of Yamada et al. [21]. With these similarities, given that the abnormal behavior of thermal physical quantities and the reduction in combustion efficiency occur due to incomplete combustion, it can be inferred that these are the same phenomenon. Additionally, a rapid increase in CO yield due to abnormal behavior can cause serious errors in fire risk assessments. Accordingly, it is necessary to closely analyze the causes of the phenomenon and changes in the internal environment.

In this context, compartment fire experiments were conducted to understand the abnormal behavior occurring in the over-ventilated condition. A 1/4 reduced-scale ISO 9705 compartment was used for the experimental apparatus. A wide range (ϕ_g = 0.2~2.0) including over- and under-ventilation conditions was considered as the GER conditions for the compartment fire experiments. In order to examine the fire characteristics across a wide GER range, the temperature and chemical species concentration inside the compartment were measured. Outside the compartment, HRR and combustion efficiency were measured, as well as the temperature and species concentration of the discharge flow through an opening. Through this, the effects and causes of abnormal phenomena occurring in the fire growth stage were analyzed.

2. Description of Experiments

Figure 1 shows a schematic diagram of the 1/4 reduced-scale ISO 9705 compartment [16] and measurement equipment. Figure 1a shows a perspective view of the experimental apparatus. The frame of the compartment was made of 5 mm thick steel, and the inside was finished with a 25 mm thick blanket-type insulator. The internal volume of the compartment installed with insulation was 0.6 m(x) × 0.9 m(y) × 0.6 m(z). A square burner with an area of 0.02 m^2 was installed at the center of the compartment floor to supply fuel. Propane, through which the supply rate can be easily adjusted, was used as the fuel in the analysis of fire phenomena by stage. To uniformly supply fuel, the burner was filled with glass beads, and the fuel flow rate was controlled using a mass flow controller. The considered experimental conditions and corresponding fuel supplies are described later. Two thermocouple trees were installed at the front and rear regions of the compartment to measure the ULT. Each thermocouple tree consisted of 11 k-type thermocouples, providing temperature measurements at 0.05 m intervals in a range of z=0.05 m to 0.55 m. The bead diameter of the thermocouples is 1.0±0.02 mm and has a bare-bead type. Bare-bead thermocouple has an error due to radiant heat in a compartment fire environment, but it can be used to understand the thermal environment of a compartment fire [24]. Plate thermometers [25] to measure incident heat flux as well as temperature were installed on the ceiling and floor of the compartment. Inhalation probes were used to measure the chemical species concentrations of the upper layer and discharge flow. Figure 1b,c show the installation locations of the probes. The high-temperature gas sampled through the probes may cause a chemical reaction while moving to the analyzer. Taking this into account, a cooling system was used to prevent the sampled gas from showing different results from the actual values in the compartment. The triple-structured probes were cooled with an average temperature of 15 °C water. The water was supplied at a sufficient flow rate (4 L/min) so that the water temperature did not greatly increase even after passing through the probe inserted into the compartment. The sampled gas passed through a copper tube installed in the ice bath, and additional cooling and moisture removal were performed in this process. The cooled gas passed through a soot filter (1 μm) and then flowed into a portable analyzer (MEXA-554JK). In this study, O_2, CO_2, CO and unburned hydrocarbons (UHC) were considered for the analysis of the chemical environment. The measurement range and accuracy of the portable analyzer used to measure the concentration of chemical species are presented in Table 1.

Figure 2 shows a schematic diagram of the various vertical opening shapes considered in this study. Incomplete combustion in the fire growth stage ended at the same time as the flame was ejected to the outside of the compartment [21]. This indicates that the start and end of this phenomenon (incomplete combustion in the fire growth stage) are closely related to the ventilation and air inflow rate through the openings. In relation to this, Yamada et al. [21] proposed a correlation equation on the abnormal behavior of combustion efficiency as a function of GER based on experimental results with various opening shapes. The GER is a variable to quantify the ventilation condition of compartment fires and can be obtained through Equation (1):

$$\mathrm{GER}\left(\phi_g\right) = \left(\gamma_s / Y_{O_2,a}\right) \times \left(\dot{m}_f / \dot{m}_a\right) \tag{1}$$

where γ_s is the mass ratio of oxygen to fuel for complete combustion, and n-heptane has a value of 3.62. $Y_{O_2,a}$ and $\dot{m}_f$ means the oxygen mass fraction in the air and fuel supply rate [kg/s]. Finally, $\dot{m}_a$ [kg/s] is the air flow rate into the compartment through an opening and is evaluated by Equation (2):

$$\dot{m}_a = 0.52A\sqrt{h} \tag{2}$$

where A and h mean the area and height of the opening. The ventilation factor of the openings in Figure 2 based on equation (2) is 0.0092 kg/s, which is the same for all.

However, according to previous studies [26,27], the ventilation factor needed to derive GER may differ from the theoretical value depending on the opening shape. Because of this, correlations [21] that do not take into account the effect of opening shape may have uncertainty. Therefore, the effect of changes in the opening shape with a fixed ventilation factor on fire characteristics should be investigated. As shown in Figure 2, openings of various shapes designed to have a constant ventilation factor were used in the experiment. The opening shapes were designed to more easily implement a wide range of GER values, including the range where abnormal behavior occurs ($\phi_g \approx 0.6$~1.2). The opening width (door width, DW) was changed to 0.10 m, 0.15 m and 0.20 m based on DW05, and the height (h) was changed to keep the ventilation factor constant. The name of each opening was determined by its width.

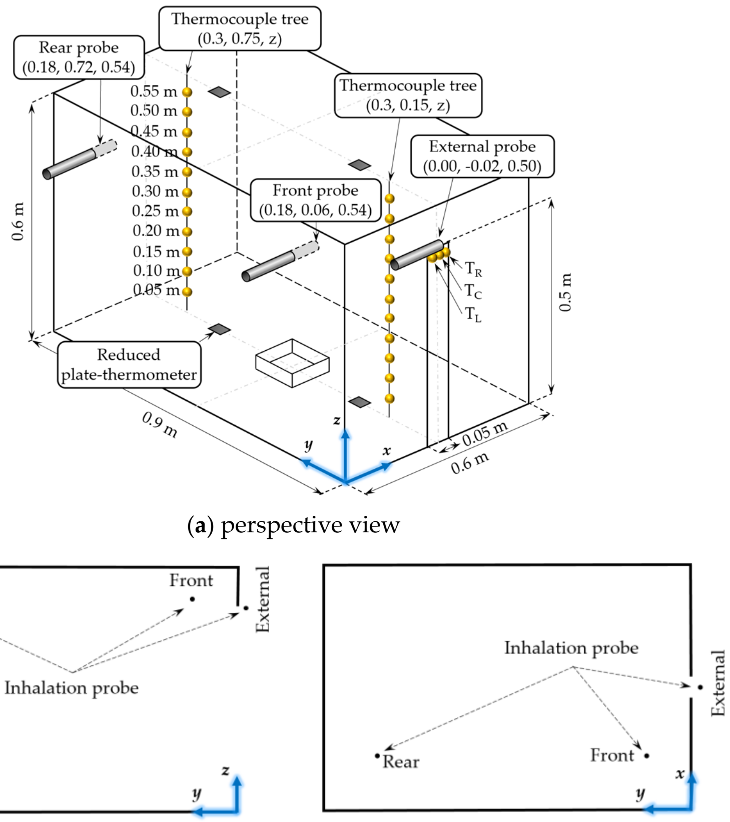

(**a**) perspective view

(**b**) side view (x=0.0 m)

(**c**) top view (z=0.6 m)

Figure 1. Schematic diagram of the 1/4 reduced-scale ISO 9705 compartment and installation location of measurement devices.

Table 1. Specification of a portable analyzer for measuring the concentration of chemical species.

	O_2	CO_2	CO	UHC
Range (%)	0–25	0–20	0–10	0–1 (10,000 ppm)
Error (%)	±0.4	±0.5	±0.06	±0.0012
Measurement method	Electrochemical sensor	Non-Dispersive Infrared (NDIR)		

Figure 3 presents a schematic diagram of the lab-scale calorimeter (LSC) [28] based on the oxygen consumption method [29,30] used to measure HRR and combustion efficiency. A square hood with a side length of 1.5 m captures combustion products and surrounding air and exhausts them through an exhaust duct (D = 0.20 m). Part of the flow passing through the exhaust duct is sampled through two porous tubes. After undergoing a pre-process to remove soot and moisture, the sampled gas is introduced into the gas analyzer

(OXYMAT 61, ULTRAMAT 23). In addition to these measurements, the HRR is calculated through the additional consideration of the mass flow rate and the average cross-sectional temperature in the exhaust duct.

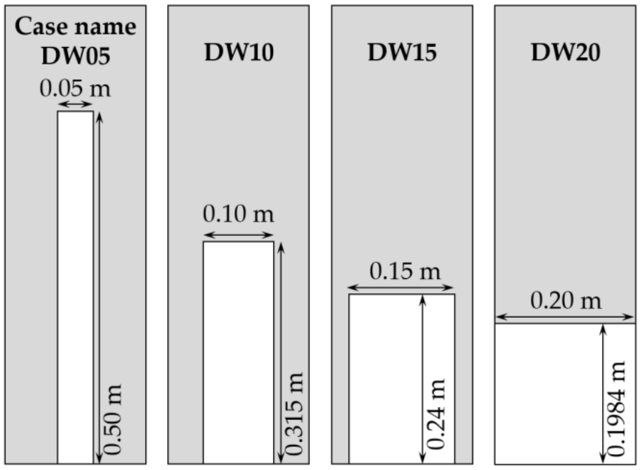

Figure 2. Schematic diagram of openings designed to have a constant ventilation factor ($0.52A\sqrt{h}$).

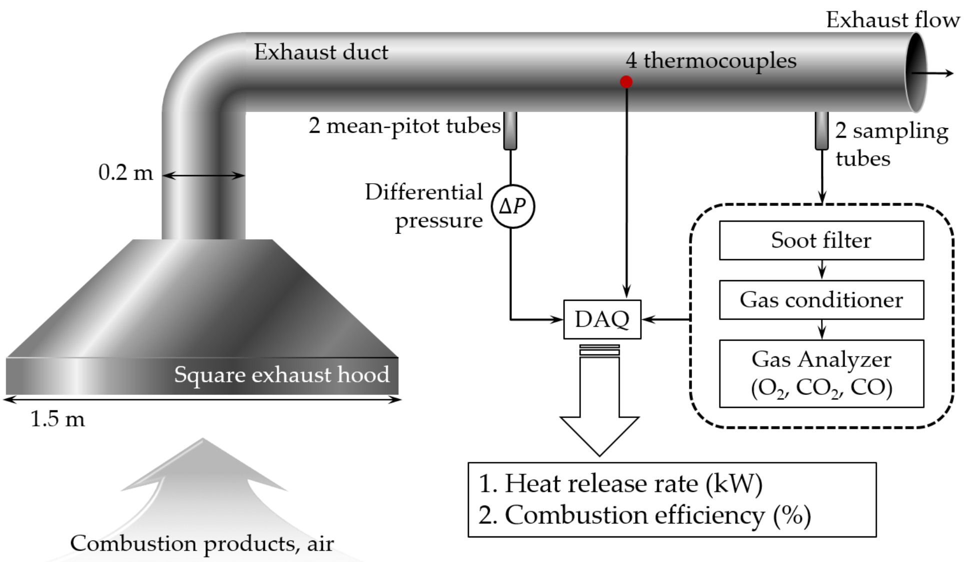

Figure 3. Lab-scale calorimeter based on the oxygen consumption method for measuring the heat release rate.

Table 2 provides a summary of the experimental conditions considered in this study and the fuel flow rate to implement each GER. At room temperature (25 °C), the ideal HRR considering fuel density (1.808 kg/m^3) and heat of combustion (46,400 kJ/kg) [31] ranges from 5.5 to 55.2 kW. Experiments for each GER were carried out for 600 to 1200 s, in which the measured HRR, temperature, incident heat flux, and species concentration reached a steady state and were sufficiently maintained. Changes in fire phenomena according to GER and opening shape were analyzed by comparing the averages at 100 s in the steady state, and the standard deviations in the form of vertical error bars were also presented.

Table 2. Summary of experimental conditions considered in the present study.

Global Equivalence Ratio (ϕ_g)	Fuel Flow Rate (L/min)	Ideal HRR (kW)
0.20	3.9	5.5
0.40	7.9	11.0
0.60	11.8	16.6
0.70	13.8	19.3
0.80	15.8	22.1
0.85	16.8	23.5
0.90	17.8	24.8
0.95	18.8	26.2
1.00	19.7	27.6
1.10	21.7	30.4
1.20	23.7	33.1
1.30	25.7	35.9
1.40	27.6	38.6
1.50	29.6	41.4
1.75	34.6	48.3
2.00	39.5	55.2

3. Numerical Details

Fire Dynamics Simulator (FDS) [32] version 6.7.0 was used for the numerical analysis of fire phenomena under experimental conditions. To minimize the error caused by boundary conditions in the numerical analysis results, including the compartment (0.6 m $\times$ 0.9 m $\times$ 0.6 m), the expanded calculation area had a size of 0.6 m $\times$ 1.8 m $\times$ 1.2 m. The physical properties of the inner walls were input with reference to the specific heat (1.088 kJ/kg·K), thermal conductivity (0.058–0.17 W/m·K), and density (128 kg/m^3) of the insulating material used in the experiments. FDS directly analyzes the governing equations for large eddies, which are responsible for most of the energy and turbulent transport in a fire environment, and for sub-grid scale eddies, large eddy simulation (LES), which applies a model, was adopted. Therefore, the accuracy of numerical analysis using FDS is closely related to the grid size (δx). This is why it is critical to select an appropriate grid size when using FDS, and grid sensitivity analysis is performed for this. When selecting the grid size for an experimental set comprising many conditions, it is effective to perform grid sensitivity analysis on the smallest-scale experiment (HRR). The smallest-scale experiment in this study is the condition ϕ_g = 0.2. Hence, a grid sensitivity analysis was conducted under the conditions of DW05 and ϕ_g = 0.2. When configuring the grid system for the grid sensitivity analysis, the characteristic fire length (D^*) concept [33] can be considered. The characteristic fire length is a dimensionless number that indicates the size of a fire source and is defined as in Equation (3):

$$D^* = \left(\frac{\dot{Q}_{max}}{\rho_\infty C_P T_\infty \sqrt{g}} \right)^{\frac{2}{5}} \quad (3)$$

where $\dot{Q}_{max}$ is the maximum HRR of the fire source. ρ_∞, C_P, T_∞, and g indicate the density (1.2 kg/m^3), specific heat (1 kJ/kg·K), and temperature (293.15 K) of the surrounding air and gravitational acceleration (9.81 m/s^2), respectively. Under room temperature 20°C and atmospheric pressure 1 atm, D^* of the condition ϕ_g = 0.2 according to Equation (1) is 0.12 m. According to previous studies [34,35], adequate predictive performance can be expected when $D^*/\delta x$ is 4 to 20. This study considered coarse (δx = 0.02 m), moderate (δx = 0.015 m), and fine (δx = 0.01 m) conditions for the grid sensitivity analysis. $D^*/\delta x$ of each grid system is 6, 8, and 12, and the total cell number is 162,000, 384,000, and 1,296,000. 1The grid sensitivity analysis using these grid systems was conducted for the ULT and chemical species concentrations (O_2, CO_2).

Figure 4 shows the grid sensitivity analysis results. In Figure 4a, in the process of increasing the temperature, the temperature measured in the experiment rises more slowly than the predicted temperature; this difference is attributed to the shape, diameter, and direction of the beads. However, the predicted and measured temperatures in the steady state, the focus of this study, exhibited similar trends. The temperatures predicted according to grid size showed the same values over all sections, indicating that the grid sensitivity to temperature was not large. In contrast, in Figure 4b, the decrease in O_2 was overestimated for the coarse condition, unlike moderate and fine. Moreover, a comparison with the experimental measurements indicated relatively large errors for coarse. In Figure 4c as well, the CO_2 volume fraction was overestimated for coarse compared with moderate and fine, with large errors in the measured values. A grid sensitivity analysis is the process of finding the conditions in which the grid size does not impact the numerical analysis results. Taking this into account, the coarse condition was not suitable to use in this study because the predicted values changed depending on the grid size and also showed a relatively large error. Considering the costs (computational resources, time) required for the numerical analysis, it was efficient to use the moderate condition. However, at higher GER conditions, the reduction in the resolution of the opening flow can cause errors in the numerical analysis results [36]. Taking this into account, the fine condition where as many grids as possible can be inserted in the opening area was used for the numerical analysis.

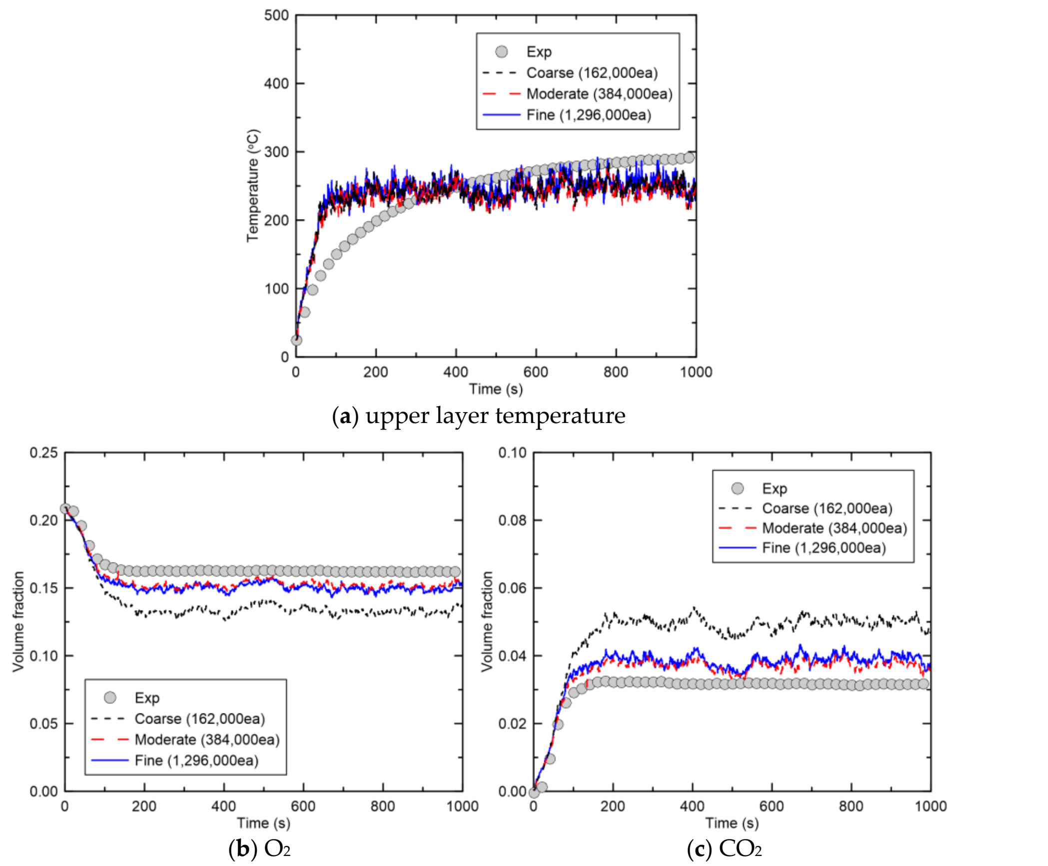

Figure 4. Results of grid sensitivity analysis for major fire physical quantities (temperature, O_2, and CO concentrations).

4. Results and Discussion

Prior to the compartment fire experiments, experiments according to fuel flow were performed in an open environment, and the results are presented in Figure 5. In the figure, the average HRR and combustion efficiency measured in the steady state for each experimental condition are presented as a function of the fuel flow rate. Except for a slight difference in the high fuel flow rate condition, the average HRR measured with the LSC showed similar behavior to the ideal HRR (solid line) according to the fuel supply. This trend was identical in the investigation of combustion efficiency. The combustion efficiency was close to 100% at a relatively low fuel flow rate but gradually decreased as the fuel flow rate increased. Nevertheless, the lowest value of combustion efficiency in an open environment is 94%, indicating that the conditions considered in this study burn very smoothly in an open environment.

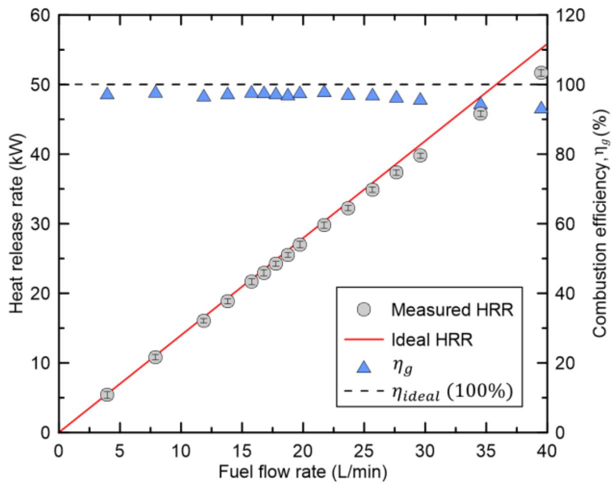

Figure 5. Heat release rate and combustion efficiency in an open environment according to the fuel supply conditions.

Figure 6 shows a comparison of instantaneous flame photos under typical GER conditions to examine the effect of the opening shape on the fire phenomenon. As confirmed in previous studies [26,27], the actual air inflow rate may differ from the theoretical value depending on the opening shape. Under identical fuel flow rate conditions, a change in air inflow rate causes a change in GER. Accordingly, in the analysis of compartment fire experiments, GER was expressed as nominal GER (ϕ_g^n) based on fuel flow rate and theoretical ventilation factor. Figure 6a–c presents photos of instantaneous flames under the over-ventilated (ϕ_g^n = 0.2), stoichiometric (ϕ_g^n = 1.0), and under-ventilated (ϕ_g^n=2.0) conditions for the DW05 opening. In Figure 6(a), the over-ventilated condition, the combustion reaction occurs only in the compartment, and the flame length is short. In the condition of ϕ_g^n = 1.0 (Figure 6b), most of the combustion reaction takes place within the compartment, but the intermittent ejection of the flame tip is observed as the flame length increases. Figure 6c corresponding to ϕ_g^n=2.0 shows the characteristics of under-ventilated condition in which flames are ejected outside the compartment. Through this, a change in the fire phenomenon according to the fuel flow rate is observed under the same opening condition. Figure 6d–e show instantaneous flame photos of different openings taken in the experiment under the condition ϕ_g^n = 1.0. Figure 6d presents a photo of DW10. This condition did not show a great difference from DW05, and only the flame tip was intermittently ejected. Figure 6e shows the DW15 experiment, in which the flame volume ejected through the opening slightly increased. Finally, Figure 6f shows the DW20 experiment, where a substantial flame volume is ejected outside the compartment even under ϕ_g^n = 1.0. Consequently, the ejected flame volume tended to increase as the width of the opening increased (as the height decreased) at the same nominal GER. This difference indicates that even if openings are designed to have a constant ventilation factor, the fire phenomena change according to the opening shape.

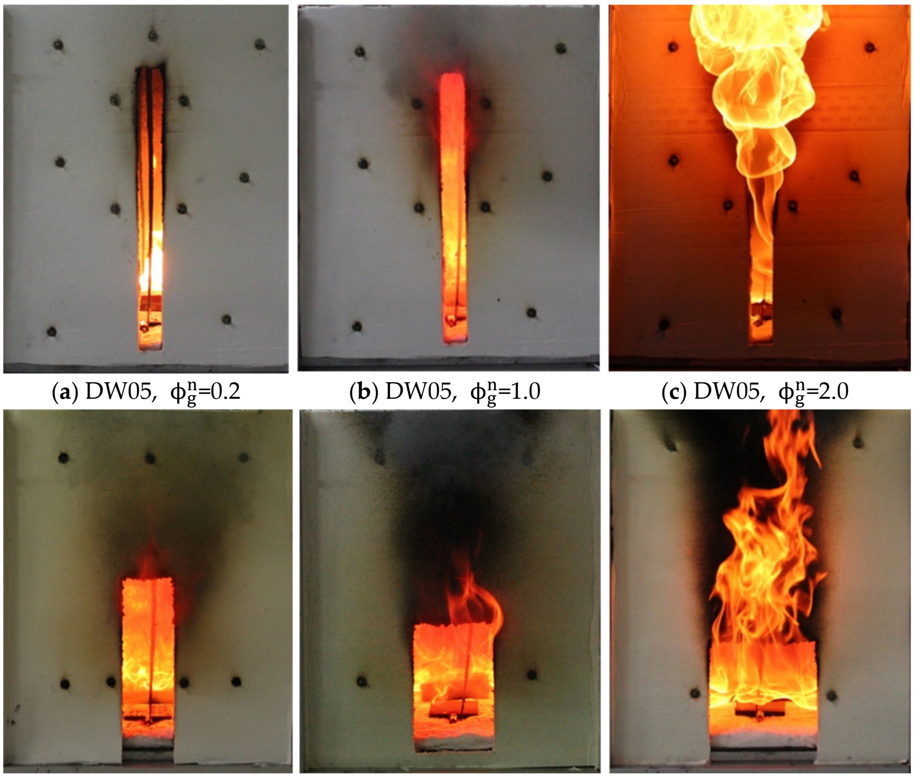

(**a**) DW05, ϕ_g^n=0.2 (**b**) DW05, ϕ_g^n=1.0 (**c**) DW05, ϕ_g^n=2.0

(**d**) DW10, ϕ_g^n=1.0 (**e**) DW15, ϕ_g^n=1.0 (**f**) DW20, ϕ_g^n=1.0

Figure 6. Comparison of instantaneous flame photos according to the opening shape in representative nominal GER (ϕ_g^n) conditions.

To investigate the internal environment according to flame behavior, Figure 7 shows a comparison of the average ULT according to nominal GER. The front and rear temperatures were measured via thermocouples installed at a height of 0.55 m from the compartment floor. When the fire source is located at the center of the compartment, the internal thermal environment undergoes the following changes as the fire grows. At a very low GER condition, the flame forms in the vertical direction of the fire source, and the front and rear temperatures do not greatly differ. As the fuel flow rate (i.e., GER) increases, the mass of combustion products and air entering and exiting the compartment also increases. At this time, the increased flow rate of the inlet causes the flame to move to the rear of the compartment, thus increasing the temperature at the rear. As GER further increases, the oxygen inside the compartment is depleted, and the flame moves to the front. In this process, the front and rear temperatures become reversed, and the front exhibits a higher temperature. From this perspective, examining the experimental results of DW05 in Figure 7a, the front and rear temperatures in the range of ϕ_g^n = 0.2 to 0.8 do not show a large difference ($T_{front} \approx T_{rear}$). However, at ϕ_g^n = 0.85, it shows a relatively high temperature at the rear side ($T_{front} < T_{rear}$). At ϕ_g^n=2.0, the temperature difference between the front and rear decreases due to the forward movement of the flame, and at a higher ϕ_g^n, the front will show a higher temperature ($T_{front} > T_{rear}$). The experimental results of the other openings in Figure 7b–d also exhibit similar behavior. However, the timing at which the relationship between the temperatures measured at the front and rear changes varies depending on the shape of the opening. The experimental results of DW10 in Figure 7b do not greatly differ from DW05. On the other hand, in the experiment of DW15, the rear temperature showed a higher value at ϕ_g^n = 0.8, and the temperatures were reversed at ϕ_g^n = 1.5. This trend is intensified in the DW20 experiment. Specifically, the rear temperature is higher than under the condition of ϕ_g^n = 0.7, and the temperature reversal is observed under the condition of ϕ_g^n = 1.1.

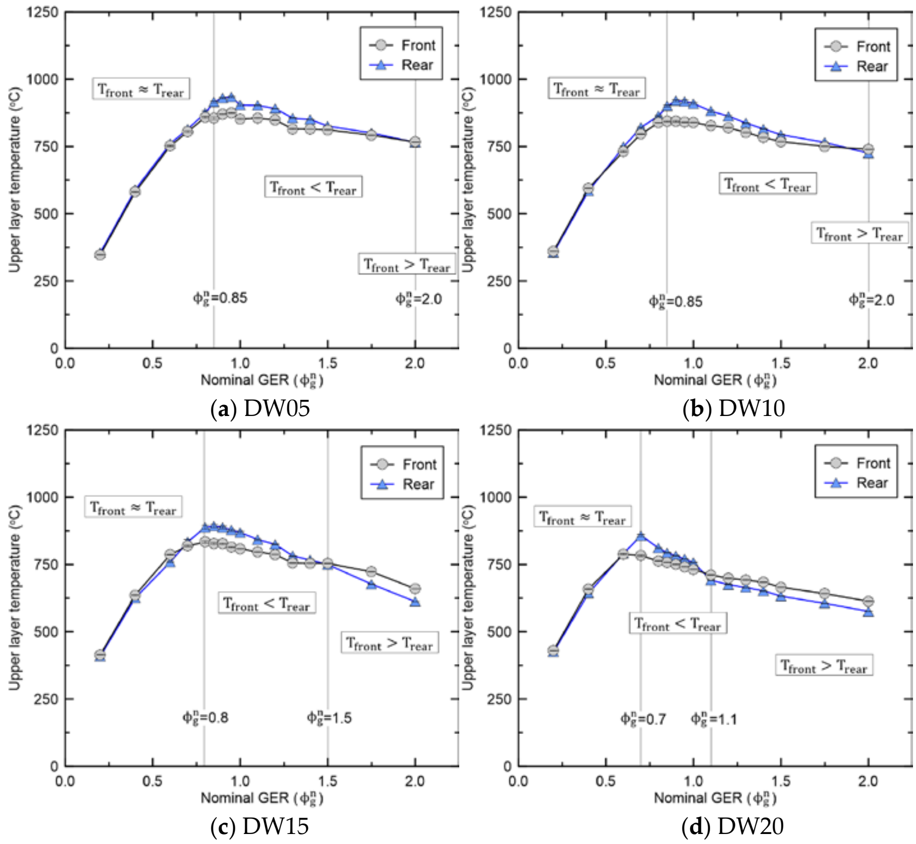

Figure 7. Average upper layer temperature of the front and rear regions in the compartment according to nominal GER (ϕ_g^n).

That is, as the opening height decreased, the thermal environment changed at a lower nominal GER. Through this, it can be seen that even if the ventilation factor is the same, the transition condition (fuel flow rate, GER) to the under-ventilated fire varies depending on the opening shape. Similarly, the same result can be obtained in comparison with the condition in which the maximum temperature is measured. In general, the temperature of the fire environment shows the maximum value under stoichiometric ($\phi_g^n = 1.0$) conditions [19]. The nominal GER at which the maximum temperature was measured in the experiment of each opening was 0.95, 0.90, 0.85, and 0.70 in the order of increasing opening width. That is, as the height of the opening decreases, the stoichiometric ratio is reached under the condition of a relatively lower fuel flow rate.

Figure 8 compares the average volume fractions of species measured in the upper layer according to the nominal GER under various opening shape conditions. Under the same nominal GER conditions, the volume fraction of O_2 decreases with decreasing opening height in Figure 8a. Conversely, CO_2 exhibits a higher volume fraction as the height of the opening decreases. Through this, it can be seen that the change in the opening shape affects the chemical environment inside the compartment under the same fuel flow condition. As a result of examining CO volume fraction (Figure 8c), under the same fuel supply condition, the lower the opening height, the higher the value, and the UHC also exhibits the same behavior with CO. In particular, the volume fraction of UHC exceeded the measurement limit under some conditions during the experiments on DW15 and DW20, which have relatively low heights. Considering that CO and UHC are incomplete combustion materials, these results mean that the lower the opening height, the more inefficient combustion occurs under the same fuel supply condition. Changes in the chemical environment according to the opening shape can lead to changes in the overall characteristics of the compartment fires. Therefore, the cause of the change in chemical environment according to the shape of the opening should be examined.

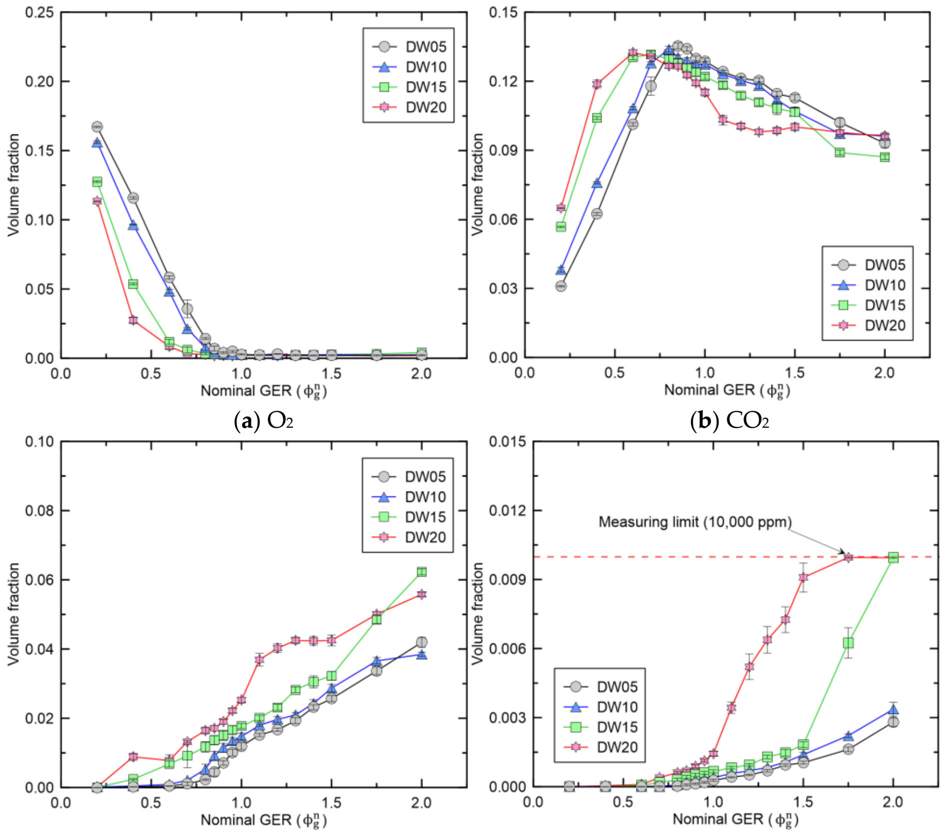

(**a**) O_2 (**b**) CO_2 (**c**) CO (**d**) UHC

Figure 8. Comparison of species (O_2, CO_2, CO and UHC) volume fraction according to opening shape at the upper layer as a function of the nominal GER (ϕ_g^n).

In order to analyze the cause of the change in the fire phenomenon according to the opening shape, Figure 9 compares the average air inflow rate in the steady state under representative nominal GER (ϕ_g^n) conditions. There are various difficulties in directly measuring air inflow through an opening. These typically include flow derangement caused by the measurement instrument, real-time changes in flow due to interaction with neutral plane height, and difficulties in deriving representative values for non-uniform flow distributions. Accordingly, Figure 9 compares the average air inflow rate in the steady state predicted through FDS. Figure 9a presents a comparison of the predicted air inflow rate according to the opening shape at ϕ_g^n = 0.2, the over-ventilated condition. As a result, although the openings had the same ventilation factor, the lower the opening height, the lower the air inflow rate. As a result of comparison under the condition of ϕ_g^n = 1, the air inflow rate was also increased for all opening shapes due to the increase in the emission of combustion products. Nevertheless, the trend of decreasing air inflow with the height of the opening was the same. This trend was also observed under the ϕ_g^n=2.0 condition (Figure 9c), which is the under-ventilated condition. The cause of the changes in fire phenomena shown in Figures 7 and 8 can be explained by these results. As the opening height decreases, the air inflow rate decreases, causing differences in the thermal and chemical environments of compartments with the same ventilation factor. This examination suggests that errors occur in the air inflow rate predicted from $0.52A\sqrt{h}$ depending on the opening shape.

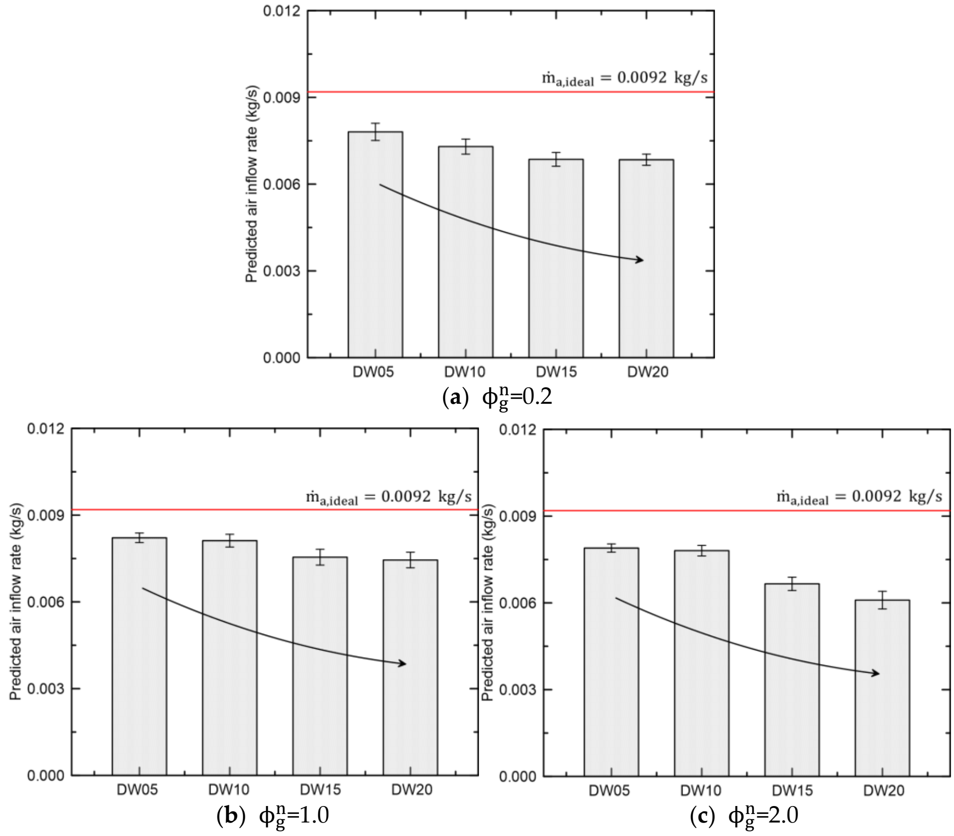

Figure 9. Comparison of predicted air inflow rate according to opening shape under various nominal GER (ϕ_g^n) conditions.

In order to examine the effect of the difference in air inflow rate on the fire phenomenon, Figure 10 compares the GER and average HRR according to the opening shape under the same fuel flow condition. In Figure 10a, the actual GER (ϕ_g) based on the air inflow rate predicted through FDS is presented as a function of the nominal GER (ϕ_g^n). As a result of the comparison, the actual GER, considering the air inflow rate according to the opening shape has a higher value than intended under all experimental conditions. Under identical fuel flow rates, actual GER increased as the opening height decreased. In particular, it was confirmed that DW20 had an actual GER exceeding 3.0 under the condition of fuel flow rate corresponding to ϕ_g^n=2.0. This difference is closely related to the change in the fire phenomenon according to the opening shape observed in Figures 6–8. Under the same fuel supply condition, a relatively high actual GER can have a very large effect on fire characteristics. Specifically, as confirmed in Figure 6, it causes an increase in the ejected flame volume and also brings a large change to the temperature distribution and chemical environment inside the compartment, as shown in Figures 7 and 8. Accordingly, actual GER (ϕ_g) considering air inflow rate for each opening shape, was used in the following analysis of fire phenomena. Figure 10b presents the average HRR in the steady state as a function of the ideal HRR. As shown in the figure, under the condition of a low ideal HRR (<20 kW), HRR does not greatly differ from the ideal HRR regardless of the opening shape. However, average HRRs in specific sections were considerably lower than the ideal HRR despite the increase in fuel flow rate. This phenomenon occurs earlier as the opening height decreases. This abnormal behavior occurs when the ideal HRR is 20–35 kW and is attributed to incomplete combustion before flame ejection as mentioned earlier.

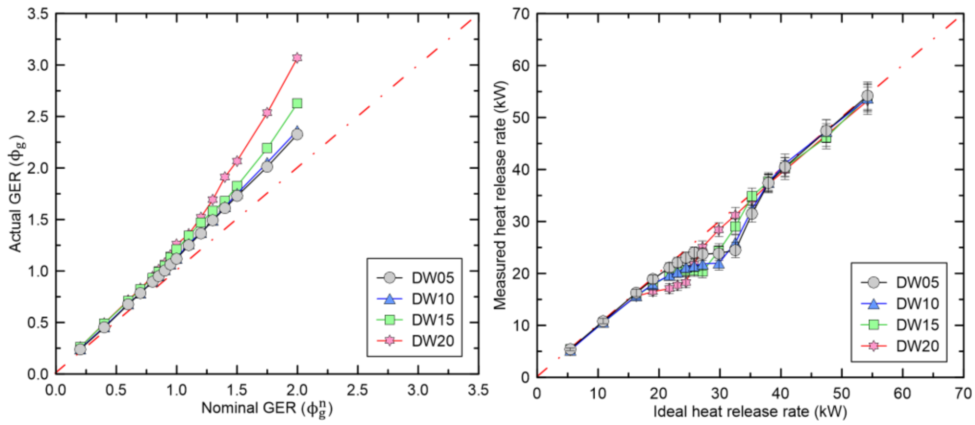

(**a**) global equivalence ratio (**b**) heat release rate

Figure 10. Change in fire phenomena according to the shape of openings with the constant ventilation factor.

Figure 11 shows the detailed analysis results of abnormal behavior according to the experimental conditions. In Figure 11a, the combustion efficiency is presented as a function of actual GER, and the combustion efficiency predicted based on the correlation proposed by Yamada et al. [21] is shown together. This study refers to the abnormal behavior of combustion efficiency caused by incomplete combustion before flame ejection as the "sinkhole phenomenon." The sinkhole phenomenon can be explained with the additional figure inserted at the top of Figure 11a. The combustion efficiency of the compartment fire under low GER conditions does not show a significant difference from that of the open environment, but the combustion efficiency begins to decrease as the GER increases. However, this decreasing trend does not continue. When GER is further increased, the sinkhole phenomenon ends, and combustion efficiency increases again. Considering this process, looking at the compartment fire experiment, the combustion efficiencies in the range of ϕ_g = 0.2~0.6 show a value close to 100% regardless of the opening shape. However, the combustion efficiency starts to decrease around ϕ_g = 0.6 and reaches a minimum of about 70%. The combustion efficiencies were compared based on the actual GER, in which the change in air inflow rate according to the opening shape was taken into account. Nevertheless, differences according to the opening shape were observed in the condition (ϕ_g) at which the decrease in combustion efficiency starts and the condition (ϕ_g) showing the lowest value. Because of this, the correlation [21] does not seem to adequately reflect the shifting of the sinkhole phenomenon along the actual GER axis according to the opening shape. These differences can be attributed to the change in the height of the neutral plane according to the opening height and the change in fuel and air mixing time due to the corresponding change in air inflow path. Therefore, the influence of these factors should be further examined to specify when the sinkhole phenomenon occurs. After showing the lowest value, the combustion efficiencies increase rapidly to reach close to 100%. The increase in combustion efficiency is achieved at the same time as the flame is ejected through the opening. Figure 11b presents actual GER (ϕ_g) at the time when the flame is first observed outside the compartment and a photo of the flame. In Figure 11a, the combustion efficiency of DW05 begins to increase at the condition with ϕ_g = 1.36, at which point flame ejection is first observed. The same phenomenon is observed in the conditions of DW10, DW15 and DW20. From these results, it can be seen that the sinkhole phenomenon has a close relationship with the flame ejection through the opening. In order to understand the relationship between flame ejection and the sinkhole phenomenon, an analysis of the opening exhaust flow according to the actual GER was performed.

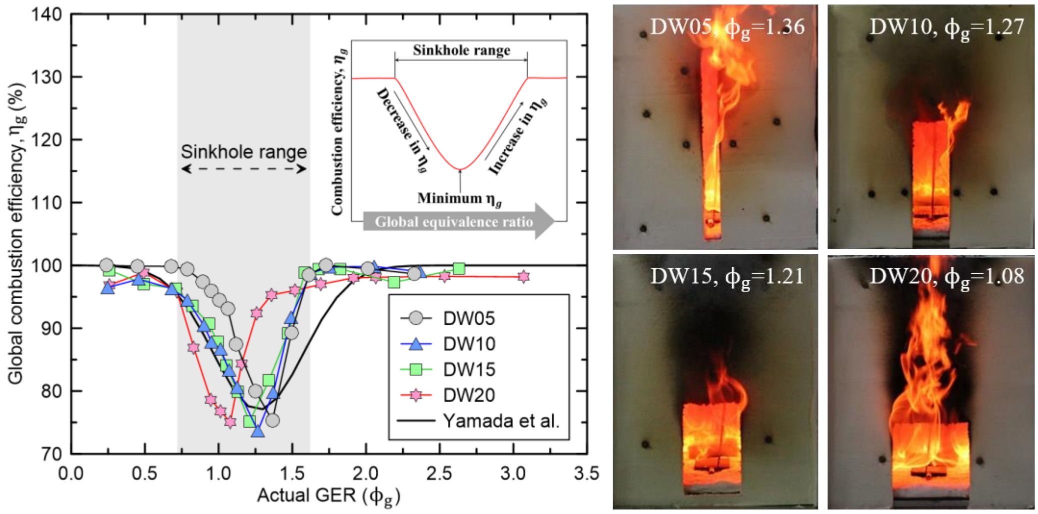

(**a**) combustion efficiency (**b**) first observation of flame ejection

Figure 11. Comparison of combustion efficiency and flame behavior according to opening shape in relation to the sinkhole phenomenon.

Figure 12 presents the measurement results of the average temperature of the discharge flow through the opening. The temperature of the discharge flow was measured through experiments on DW05, and the measurement results were presented as a function of the actual GER. The location of thermocouples (T_C, T_R and T_L) for temperature measurement is shown in Figure 1. The three thermocouples are useful for considering the temperature deviation in the width direction of the opening. Figure 12 shows the average value and standard deviation for the three measurements. In the conditions before the sinkhole phenomenon occurs, the temperature of the discharge flow increases with GER. This behavior is the same as the result of a study [19] showing that the temperature of the fire flow field increases with GER in the over-ventilated fire condition. However, in the region where the sinkhole phenomenon occurs (shaded region), the temperature of the discharge flow shows abnormal behavior. In the section where the combustion efficiency decreases (ϕ_g = 0.9~1.36), the temperature of the discharge flow does not change significantly despite the increase in the fuel flow rate. Through this, it can be seen that the amount of heat released inside the compartment is limited for some reason, and some of the supplied fuel is not burned. After that, starting with the condition of ϕ_g = 1.36 where the flame was ejected out of the compartment, the temperature of the discharge flow increased. Because the temperature inside the compartment decreased under the same conditions (Figure 7a), the temperature increase of the discharge flow is attributed to contact between the ejection flame and the thermocouple beads. To verify whether some fuel was not burned in the section where the temperature of the discharge flow did not increase, the chemical composition of the discharge flow was analyzed.

Figure 13 shows the concentration measurements of chemical species contained in the discharge flow in the DW05 experiments. In Figure 13(a), the O_2 concentration in the section where the combustion efficiency decreases remains constant and then decreases from when the flame is ejected. This indicates that the amount of fuel burned in the compartment is limited in the section where the combustion efficiency decreases. Moreover, in Figure 13b, the CO_2 concentration in the same section does not increase but slightly decreases. This behavior is attributed to the dilution effect of CO and UHC (products of incomplete combustion), along with the limitation of the combustion reaction occurring in the compartment. As shown in Figure 13c,d, the volume fractions of CO and UHC continuously increase from the time the sinkhole range is entered. The concentrations of O_2 and CO_2 do not greatly change, whereas the concentrations of CO and UHC increase, indicating that the amount of incomplete combustion continuously increases. In conclusion, it can be seen that the sinkhole phenomenon occurs because the residual fuel discharged out of the compartment after local fuel/air mixing and combustion in a real fire environment does not reach the lower combustion limit. Considering this, the reason why the actual GER exceeds 1 in the condition where the flame is first ejected in Figure 11b can be interpreted. Even in a real compartment environment, if fuel and air burn in a perfect mixture, the flame will be ejected to the outside under the condition of ϕ_g = 1. However, in the actual compartment environment, a phenomenon different from the theory is observed because flames are ejected after the concentration of the fuel discharged to the outside of the compartment reaches the lower flammable limit. When the combustion reaction does not start outside the compartment despite an increased fuel flow rate, the combustion efficiency continuously decreases. However, when the concentration of the incompletely combusted material contained in the discharge flow reaches the lower flammability limit, the combustion reaction starts outside the compartment. At this time, the incompletely combustion material comes in contact with sufficient oxygen from the outside and combusts, thus increasing the combustion efficiency. Unfortunately, the lower flammability limit has not been quantitatively evaluated because it is impossible to specify the types of incompletely burned materials contained in the discharge flow. According to the results of this study, the sinkhole phenomenon occurs in over-ventilated conditions. However, as mentioned earlier, to specify when the sinkhole phenomenon occurred, it is necessary to comprehensively consider the influence of the neutral plane height according to opening shape and the resulting change in mixing time. The sinkhole phenomenon leads to fire characteristics considerably different from those expected given the fuel supply; in particular, it generates more incompletely combusted material (CO and UHC) than under higher GER conditions. In this case, the fire may have a higher risk than is predicted based on generally accepted knowledge and may cause an increase in human life and property damage due to an inadequate response. Therefore, changes in fire characteristics due to the sinkhole phenomenon should be considered when performing a fire risk assessment. In addition, a follow-up study to specify the occurrence range of the sinkhole phenomenon is required.

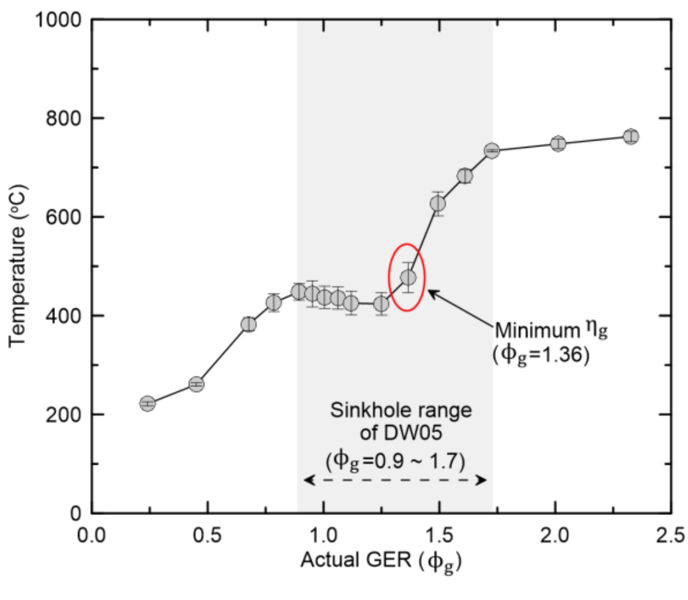

Figure 12. Average temperature of discharge flow measured according to actual GER (ϕ_g) in experiments on the DW05 opening.

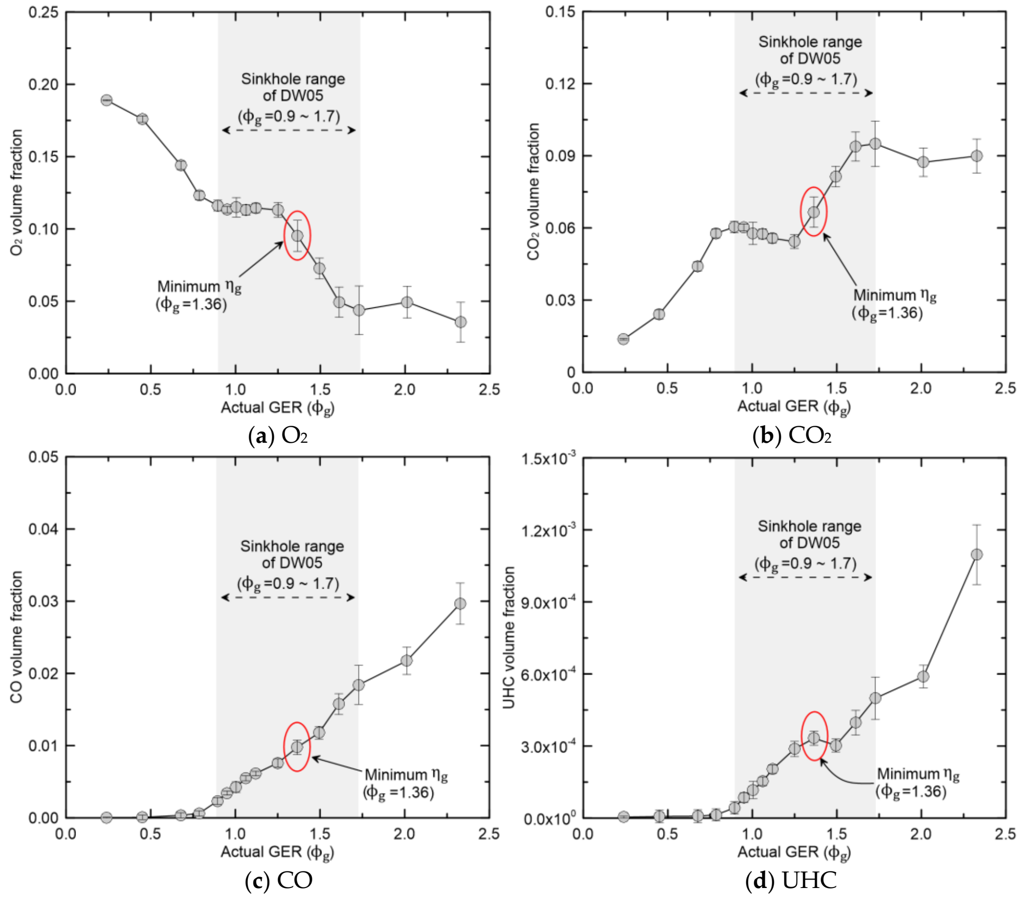

Figure 13. Measurement results of chemical species volume fraction contained in the discharge flow.

5. Conclusions

This study conducted an experimental investigation to analyze the causes of the sinkhole phenomenon, which led to abnormal behavior of heat release rate and combustion efficiency, and evaluate the influence of opening shape on fire phenomena. For this purpose, the ISO 9705 compartment reduced to 1/4 scale was utilized, and a wide range of global equivalence ratios, including over- and under-ventilated fire conditions, were considered. To analyze the fire characteristics according to the global equivalence ratio and the opening shape, the heat release rate, temperature, and chemical species concentration were measured. The conclusions of the present study are as follows:

(1) The air inflow rate varied with the shape of openings designed to have a constant ventilation factor. Consequently, under identical ventilation factor and fuel supply conditions, the thermal and chemical environment inside the compartment considerably differed according to the opening shape. To accurately understand compartment fire phenomena, theories for predicting air inflow rates must be improved.

(2) The cause of the sinkhole phenomenon was analyzed through the measurement of the temperature and the chemical species concentration of the discharge flow. The sinkhole phenomenon occurs because the fuel that is not burned due to the local combustion reaction occurring inside the compartment does not reach the lower flammable limit even outside the compartment. The sinkhole phenomenon ended simultaneously with the combustion reaction outside the compartment, i.e., flame eruption.

(3) The sinkhole phenomenon caused by incomplete combustion in the over-ventilated condition leads to a higher fire risk than predicted. In particular, the generation of toxic substances due to incomplete combustion poses a huge threat to human safety, so this must be considered in fire risk assessments.

Author Contributions: Conceptualization, S.-Y.M., H.-S.Y. and C.-H.H.; methodology, S.-Y.M., H.-S.Y. and C.-H.H.; validation, H.-S.Y. and C.-H.H.; formal analysis, H.-S.Y.; investigation, S.-Y.M. and H.-S.Y.; resources, S.-Y.M., H.-S.Y. and C.-H.H.; data curation, H.-S.Y.; writing—original draft preparation, H.-S.Y.; writing—review and editing, H.-S.Y. and C.-H.H.; supervision, C.-H.H.; All authors have read and agreed to the published version of the manuscript.

Funding: This paper was supported by the "National Fire Agency" R&D program (20016433).

Institutional Review Board Statement: Not applicable.

Informed Consent Statement: Not applicable.

Data Availability Statement: The data used to support the findings of this study are available from the corresponding author upon request.

Conflicts of Interest: The authors declare no conflict of interest.

References

1. Hwang, C.H.; Lock, A.; Bundy, M.; Johnsson, E.; Ko, G.H. Studies on Fire Characteristics in Over-and Under ventilated Full-Scale Compartments. *J. Fire Sci.* **2010**, *28*, 459–486.
2. Peatross, M.J.; Beyler, C.L. Ventilation Effects on Compartment Fire Characterization. In Proceedings of the 5th International Symposium on Fire Safety Science, World Congress Centre, Melbourne, Australia, 3–7 March 1997.
3. Hitomo, K.; Tsuchihashi, T.; Tanaka, Y.; Tanaka, T. Modeling thermal behaviors of window flame ejected from a fire compartment. *Fire Saf. J.* **2009**, *44*, 230–240.
4. Delichatsios, M.A. Enclosure and Façade fires: Physics and applications. In Proceedings of the 11th International Symposium on Fire Safety Science, Christchurch, New Zealand, 9–14 February 2014.
5. Hu, L.; Hu, K.; Ren, F.; Sun, X. Facade flame height ejected from an opening of fire compartment under external wind. *Fire Saf. J.* **2017**, *92*, 151–158.
6. Lulea, M.D.; Iordache, V.; Năstase, I. Experimental and Numerical Study on the Influence of Mechanical Ventilation on the Survival Conditions in a Room Set on Fire. *Math. Model. Civ. Eng.* **2021**, *16*, 45–63.
7. Johansson, N.; Hees, P.V. A Correlation for Predicting Smoke Layer Temperature in a Room Adjacent to a Room Involved in a Pre-Flashover Fire. *Fire Mater.* **2014**, *38*, 182–193.
8. Gottuk, D.T.; Roby, R.J.; Beyler, C.L. A Study of Carbon Monoxide and Smoke yields from Compartment Fires with External Burning. In Proceedings of the 24th International Symposium on Combustion, Sydney, Australia, 5–10 July 1992.
9. Stec, A.A.; Hull, T.R.; Purser, D.A.; Purser, J.A. Fire Toxicity Assessment: Comparison of Asphyxiant Yields From Laboratory and Large Scale Flaming Fires. In Proceedings of the 11th International Symposium on Fire Safety Science, Christchurch, New Zealand, 9–14 February 2014.
10. Hu, L.; Qui, Z.; Lu, K.; Tang, F. Window Ejected Flame Width and Depth Evolution Along Façade From Under-Ventilated Enclosure Fires. *Fire Saf. J.* **2015**, *76*, 44–53.
11. Asimakopoulou, E.K.; Chotzoglou, K.; Kolaitis, D.I.; Founti, M.A. Characteristics of Externally Venting Flames and Their Effect on the Facade: A Detailed Experimental Study. *Fire Technol.* **2016**, *52*, 2043–2069.
12. Lock, A.; Bundy, M.; Johnsson, E.L.; Hamins, A.; Ko, G.H.; Hwang, C.H.; Fuss, P.; Harris, R. Experimental Study of the Effects of Fuel Type, Fuel Distribution, and Vent Size on Full-Scale Underventilated Compartment Fires in an ISO 9705 Room. NIST Technical Note 1603, Gaithersburg, Maryland, USA. 2008. Available online: https://tsapps.nist.gov/publication/get_pdf.cfm?pub_id=861620 (accessed on 21 November 2022).
13. Hwang, C.H.; Lock, A.; Bundy, M.; Johnsson, E.; Ko, G.H. Effects of Fuel Location and Distribution on Full-Scale Underventilated Compartment Fires. *J. Fire Sci.* **2011**, *29*, 21–52.
14. Parkes, A.R. The Impact of Size and Location of Pool Fires on Compartment Fire Behaviour. Ph.D. Thesis, University of Canterbury, Christchurch, New Zealand, 2009.
15. Bjorn, K.; Quintiere, J. *Enclosure Fire Dynamics*; CRC Press: Boca Raton, FL, USA, 1999; Chapter 6.3.
16. *ISO 9705-1:1993*; Fire tests—Full-Scale Room Test for Surface Products. International Organization for Standardization: Geneva, Switzerland, 1993.
17. Pitts, W.M. The global equivalence ratio concept and the formation mechanism of carbon monoxide in enclosure fire. *Prog. Energy Combust. Sci.* **1995**, *21*, 197–237.
18. Gottuk, D.T.; Roby, R.J.; Peatross, M.J.; Beyler, C.L. Carbon monoxide production in compartment fires. *J. Fire. Prot. Eng.* **1992**, *4*, 133–150.
19. Hwang, C.H.; Park, C.H.; Ko, G.H.; Lock, A. An Experimental Study on Relationship Between Global Equivalence Ratio and Fire Characteristics in Full-Scale Compartment Fires. *J. Korean Soc. Combust.* **2010**, *15*, 32–39.
20. Ko, G.H.; Park, C.H.; Hwang, C.H.; Park, S.H. A Study on the Combustion Efficiency Concept in Under-ventilated Compartment Fires. *Fire Sci. Eng.* **2010**, *24*, 145–152.

21. Yamada, T.; Takanashi, K.; Yanai, E.; Suzuki, T. An Experimental Study of Ejected Flames and Combustion Efficiency. In Proceedings of the 7th International Symposium on Fire Safety Science, Worcester, MA, USA, 16–21 June 2002.
22. Lee, Y.P.; Delichatsios, M.A.; Silcock, G.W.H. Heat Fluxes and Flame Heights in Facades from Fires in Enclosures of Varying Geometry. *Proc. Combust. Inst.* **2007**, *31*, 2521–2528.
23. Ukleja, S.; Delichatsios, M.A.; Delichatsios, M.M.; Lee, Y.P. Carbon Monoxide and Smoke Production Downstream of a Compartment for Underventilated Fires. In Proceedings of the 9th International Symposium on Fire Safety Science, Karlsruhe, Germany, 21–26 September 2008.
24. Han, H.S.; Yun, H.S.; Hwang, C.H.; Kim, S.C. An Experimental Study on Temperature Measurement Bias using Thermocouple in Simulated Thermal Environments of Fire. *J. Korean Soc. Saf.* **2017**, *32*, 7–13.
25. *ISO 834—1:1999*; Fire resistance tests—Elements of building construction—Part 1: General requirements. International Organization for Standardization: Geneva, Switzerland, 1999.
26. Mun, S.Y. Experimental and Numerical Studies on Effects of Opening Configuration on the Fire Characteristics in a Compartment. Master's Thesis, Daejeon University, Deajeon, Republic of Korea, 2014.
27. Yun, H.S. A Study on the Variation of Fire Characteristics according to the Internal Volume of the Compartment and Ventilation Area. Master's Thesis, Daejeon University, Deajeon, Republic of Korea, 2017.
28. Yun, H.S. Methodology for Predicting Heat Release Rate and CO Yield of Compartment Fires Using Fire Characteristics in an Open Environment. Ph.D. Dissertation, Daejeon University, Deajeon, Republic of Korea, 2022.
29. Thornton, W.M. The Relation of Oxygen to the Heat of Combustion of Organic Compounds. *Philos. Mag. J. Sci.* **1917**, *33*, 196–203.
30. Huggett, C. Estimation of Rate of Heat Release by Means of Oxygen Consumption Measurements. *Fire Mater.* **1980**, *4*, 61–65.
31. National Fire Protection Association. *SFPE Handbook of Fire Protection Engineering*, 3rd ed.; NFPA Press: Boston, MA, USA, 2002; pp. 2–192.
32. McGrattan, K.; McDermott, R.; Weinschernk, C.; Floyd, J.; Weinschenk, C.; Overholt, K. *Fire Dynamics Simulator User's Guide*, 6th ed.; NIST SP 1019; NIST: Gaithersburg, MD, USA, 2017.
33. Bounagui, A.; Benichou, N.; McCartney, C.; Kashef, A. Optimizing the Grid Size Used in CFD Simulations to Evaluate Fire Safety in Houses. In Proceedings of the 3rd NRC Symposium on Computational Fluid Dynamics, High Performance Computing and Virtual Reality, Ottawa, ON, Canada, 4 December 2003.
34. McGrattan, K.; Floyd, J.; Forney, G.; Baum, H. Improved Radiation and Combustion Routines for a Large Eddy Simulation Fire Model. In Proceedings of the 7th International Symposium on Fire Safety Science, Worcester, MA, USA, 16–21 June 2002.
35. McGrattan, K. *Verification and Validation of Selected Fire Models for Nuclear Power Plant Applications: Fire Dynamics Simulator (FDS) (NUREG-1824 and EPRI 1011999)*; U.S. Nuclear Regulatory Commission: Rockville, MD, USA, 2007. Available online: https://www.nrc.gov/reading-rm/doc-collections/nuregs/staff/sr1824/v7/index.html (accessed on 21 November 2022).
36. Mun, S.Y.; Hwang, C.H. Performance Evaluation of FDS for Predicting the Unsteady Fire Characteristics in a Semi-Closed ISO 9705 Room. *Fire Sci. Eng.* **2012**, *26*, 21–28.